

Electroweak Matrix Elements in the Two-Nucleon Sector from Lattice QCD

William Detmold and Martin J. Savage

Department of Physics, University of Washington, Seattle, WA 98195-1560.

Abstract

We demonstrate how to make rigorous predictions for electroweak matrix elements in nuclear systems directly from QCD. More precisely, we show how to determine the short-distance contributions to low-momentum transfer electroweak matrix elements in the two-nucleon sector from lattice QCD. In potential model descriptions of multi-nucleon systems, this is equivalent to uniquely determining the meson-exchange currents, while in the context of nuclear effective field theory, this translates into determining the coefficients of local, gauge-invariant, multi-nucleon-electroweak current operators. The energies of the lowest-lying states of two nucleons on a finite volume lattice with periodic boundary conditions in the presence of a background magnetic field are sufficient to determine the local four-nucleon operators that contribute to the deuteron magnetic moment and to the threshold cross-section of $np \rightarrow d\gamma$. Similarly, the energy-levels of two nucleons immersed in a background isovector axial weak field can be used to determine the coefficient of the leading local four-nucleon operator contributing to the neutral- and charged-current break-up of the deuteron. This is required for the extraction of solar neutrino fluxes at SNO and future neutrino experiments.

November 1, 2018

I. INTRODUCTION

A major goal of nuclear physics is to be able to rigorously compute the properties and interactions of nuclei directly from QCD. While QCD is formulated in terms of quarks and gluons, the relevant degrees of freedom of strongly interacting systems probed at low-momentum are the lowest-lying hadrons. While the properties of these hadrons are well known experimentally, and some of their interactions are also well studied (such as the nucleon-nucleon (NN) cross-section), in general, direct measurement of the interactions that contribute to nuclear processes is not possible. For instance, there are multi-nucleon interactions induced at the chiral symmetry breaking scale, that will not be directly measured, but which contribute to the interactions of nuclei. The only way of rigorously computing strong interaction observables and electroweak observables involving hadrons, is with lattice QCD. In lattice QCD space-time is discretized and Green functions are evaluated in Euclidean space. At this point in time the variety of processes that can be addressed with lattice QCD is quite limited. Present day computational power restricts the sizes of lattices, the lattice spacings, and the quark masses that can be used in simulations, making the extraction of physical observables non-trivial.

Even if infinite computing power were to become available tomorrow most of the formal framework with which to calculate most nuclear properties and observables does not yet exist. Notable exceptions are the NN and nucleon-hyperon (NY) scattering lengths and range parameters [1, 2, 3, 4, 5]. At the heart of the issue is the Maiani-Testa theorem [6] which precludes determination of scattering amplitudes from Euclidean-space Green functions at infinite volume away from kinematic thresholds. By generalizing a result from non-relativistic quantum mechanics [1] to quantum field theory, Lüscher [2, 3] showed how to extract the $2 \rightarrow 2$ scattering amplitude from the energy-levels of two particles in a finite-volume lattice simulation. This technique has been used to determine the low-energy $\pi\pi$ phase shifts directly from QCD, e.g. Ref. [7]. However, only one lattice QCD calculation of the NN scattering lengths [8] exists, and it is quenched with relatively large quark masses (for a review see Ref. [9]).

In this work we establish a framework with which to extract the electroweak matrix elements in the two-nucleon sector. This is only a small step toward a framework with which to determine electroweak matrix elements in arbitrary multi-nucleon systems, however, the two-nucleon sector is pleasantly challenging all by itself. Naively this appears to require the computation of hadronic five-point correlators, a daunting task that is beyond the reach of current computers. However, calculation of the energy-levels of two nucleons in a finite volume in the presence of appropriate background electroweak fields allows for these matrix elements to be extracted with little more computing resources than are needed to calculate the scattering parameters. We start by studying the energy-levels of two nucleons immersed in a background magnetic field. Clearly a calculation of the deuteron electromagnetic properties will not be heralded as a major accomplishment (though it would be an impressive test of lattice QCD) as they are well-known from precise experiments, e.g. Ref. [10]. However, they do provide an illustration of how the long-distance and short-distance contributions can be isolated with lattice QCD. This technique is then generalized to weak background fields in order to allow for calculation of the axial matrix element that dominates νd break-up [11, 12, 13], the process used by SNO [14] to determine the flavor composition of the solar neutrino flux. The present-day uncertainty in this matrix element will provide a significant uncertainty in the determination of neutrino mass differences and mixing matrix derived

from future experiments.

Determinations of the electroweak matrix elements will be independent of the hadronic theory used to compute the infrared (IR) properties of QCD as long as it is a complete theory consistent with all the symmetries of QCD. In this work we use effective field theory (EFT), and in particular, the pionless EFT, $\text{EFT}(\pi)$ to study the very low-momentum ($|\mathbf{p}| \ll m_\pi$) interaction of nucleons and electroweak gauge fields [15, 16, 17, 18]. $\text{EFT}(\pi)$ has been developed over the last few years to describe systems with unnaturally large scattering lengths, as are found in the multi-nucleon sector of QCD. Such large scattering lengths result from a fine-tuning that nature has presented to us, more than likely for anthropic reasons, and as a result, the analysis in this work will not apply for arbitrary values of the light-quark masses.

II. ELECTROMAGNETIC OBSERVABLES IN THE TWO-NUCLEON SECTOR AND “MESON-EXCHANGE CURRENTS”

In the traditional approach to calculating electroweak observables in nuclear physics, one assumes that all processes are dominated by one-nucleon interactions with the electroweak probe, and that multi-nucleon contributions are small. These multi-nucleon interactions result from currents coupling to the exchange of single mesons, π ’s, ρ ’s and so forth, the same mesons that are used to construct nucleon-nucleon potentials¹ and are called “meson-exchange currents” (MEC’s)². In the context of EFT, these matrix elements receive contributions from one-nucleon interactions with the electroweak current, from interactions with the mesons that have masses below the cut-off of the theory (in the pionless theory there are no mesonic contributions, while in the pionful theory there are contributions from pions) and from local, two- (or more) nucleon – electroweak current interactions. These multi-nucleon interactions result from the physics at momentum scales above the cut-off of the EFT that has been integrated out. A significant advantage of the EFT is that no attempt is made to force these interactions to look like they result from the exchange of mesons – they are what they are. However, before the EFT can become predictive, the coefficients of the various operators that occur in it must be determined either from experiment or from lattice QCD.

As the scattering lengths in both the 1S_0 and 3S_1 channels ($a_1 = -23.714$ fm and $a_3 = 5.425$ fm) are unnaturally large (both channels are near their IR fixed-points [15, 16, 19, 20]), $\text{EFT}(\pi)$ can even be used to describe electroweak processes involving the deuteron. $\text{EFT}(\pi)$ can be recast into a somewhat simpler theory with which to perform computations up to a given order in the momentum expansion by introducing dynamical di-baryon fields [21, 22]. As S-matrix elements calculated in the usual formulation of $\text{EFT}(\pi)$ and with the di-baryon formalism are the same at any given order in the expansion and the two frameworks differ only in the ultra-violet (UV), both forms will give identical results for observables in a finite-volume.

In this work we will not reproduce the methodology of $\text{EFT}(\pi)$ [18], however, we shall

¹ The modern potentials that best fit all available data, e.g. AV_{18} , do not rely on single meson exchange to describe the short-distance component of the NN potential, instead use some “best-fit” functional forms that minimize the χ^2/dof of the fit to NN data.

² Of course, this terminology assumes that all interactions can be represented by meson exchange, which while true in the large- N_C limit of QCD, is not true in general.

discuss relevant aspects of the di-baryon formalism [21, 22]. In terms of nucleon and di-baryon degrees of freedom, the leading order (LO) low-energy strong interactions for $|\mathbf{p}| \ll m_\pi/2$ are described by a Lagrange density of the form

$$\begin{aligned} \mathcal{L} = & N^\dagger \left[i\partial_0 + \frac{\nabla^2}{2M} \right] N - t_j^\dagger \left[i\partial_0 + \frac{\nabla^2}{4M} - \Delta_3 \right] t^j - s_a^\dagger \left[i\partial_0 + \frac{\nabla^2}{4M} - \Delta_1 \right] s^a \\ & - y_3 \left[t_j^\dagger N^T P_3^j N + \text{h.c.} \right] - y_1 \left[s_a^\dagger N^T P_1^a N + \text{h.c.} \right] , \end{aligned} \quad (1)$$

where N is the nucleon annihilation operator, t^j is the 3S_1 di-baryon annihilation operator with spin-index j , and s^a is the 1S_0 di-baryon annihilation operator with isospin-index a . Further, P_3^j is the spin-isospin projector for two nucleons in the 3S_1 channel with spin-index j , while P_1^a is the spin-isospin projector for two nucleons in the 1S_0 channel with isospin-index a ,

$$P_3^j = \frac{1}{\sqrt{8}} \tau_2 \otimes \sigma_2 \sigma^j , \quad P_1^a = \frac{1}{\sqrt{8}} \tau_2 \tau^a \otimes \sigma_2 . \quad (2)$$

In the Lagrange density in eq. (1), a factor of the nucleon mass M has been absorbed into the definition of the nucleon fields and similarly a factor of $2M$ into the di-baryon fields. The S-wave interactions are enhanced by a factor of the expansion parameter, $1/Q$, and are treated non-perturbatively. However the interactions that introduce mixing with higher partial waves, e.g. ${}^3S_1 - {}^3D_1$ mixing, are suppressed by at least Q^2 and so only S-wave to S-wave interactions are required to the order we are working ³. In order to recover the scattering amplitudes in both S-wave channels, the constants that appear in eq. (1) are [21]

$$y_3^2 = \frac{8\pi}{M^2 r_3} , \quad y_1^2 = \frac{8\pi}{M^2 r_1} , \quad \Delta_3 = \frac{2}{M r_3} \left(\frac{1}{a_3} - \mu \right) , \quad \Delta_1 = \frac{2}{M r_1} \left(\frac{1}{a_1} - \mu \right) \quad (3)$$

where μ is the renormalization scale, a_3 and r_3 are the scattering length and effective range in the 3S_1 channel, and a_1 and r_1 are the scattering length and effective range in the 1S_0 channel.

For the processes under consideration, the local, gauge-invariant, electroweak interactions between two-nucleons and the gauge fields need to be included in addition to the interactions that result from gauging the Lagrange density in eq. (1). The additional electromagnetic gauge-invariant operators that contribute to the processes of interest at LO and NLO in the power-counting are [22, 23]

$$\begin{aligned} \mathcal{L} = & \frac{e}{2M} N^\dagger [\kappa_0 + \kappa_1 \tau^3] \boldsymbol{\sigma} \cdot \mathbf{B} N - \frac{e}{M} \left(\kappa_0 - \frac{\tilde{l}_2}{r_3} \right) i\epsilon_{ijk} t_i^\dagger t_j B_k \\ & + \frac{el_1}{M\sqrt{r_1 r_3}} \left[t_j^\dagger s_3 B_j + \text{h.c.} \right] , \end{aligned} \quad (4)$$

where $\kappa_p = \kappa_0 + \kappa_1$ and $\kappa_n = \kappa_0 - \kappa_1$ are the proton and neutron magnetic moments, e is the electric charge, and \mathbf{B} is the magnetic field. The magnetic moment interaction of the

³ The analysis would become far more involved if this suppression was not present – see Ref. [37].

3S_1 di-baryon is written in such a way that if $\tilde{l}_2 = 0$ the deuteron magnetic moment is the sum of the neutron and proton magnetic moments [18, 21, 22, 23] (at NLO)

$$\mu_d = \frac{e}{M} \left(\kappa_0 + \frac{\gamma_0}{1 - \gamma_0 r_3} \tilde{l}_2 \right) , \quad (5)$$

where γ_0 is the binding momentum of the deuteron in an infinite volume with no background fields, and satisfies the truncated effective range expansion,

$$\gamma_0 - \frac{1}{a_3} - \frac{1}{2} r_3 \gamma_0^2 = 0 , \quad (6)$$

where the deuteron energy is $E = -\gamma_0^2/M$. As spin-dependent interactions are suppressed in the infrared, \tilde{l}_2 is expected to be small and this is verified experimentally. To make some connection with traditional nuclear physics, the constants \tilde{l}_2 and l_1 correspond to multi-nucleon interactions with the electromagnetic field induced by MEC's.

The breakdown scale of EFT($\not{\pi}$) restricts the magnitude of electroweak fields that can be described. In order to have a convergent expansion, the magnetic field must be less than $|e\mathbf{B}| \ll 2m_\pi M \sim 10^5 \text{ MeV}^2$ so that the one-nucleon magnetic moment interaction shifts the nucleon mass by less than m_π . Further, requiring that the nucleon magnetic polarizability shifts the nucleon mass by less than the magnetic moment (see eq. (7) below) requires that $4\pi \frac{\beta_{p,n}}{2} B_0^2 \ll \mu_{p,n} B_0$. Using the experimental values of $\beta_p = 1.2 \pm 0.7 \pm 0.3 \pm 0.4 \times 10^{-4} \text{ fm}^3$ and $\beta_n = 6.5 \pm 2.4 \pm 3.0 \times 10^{-4} \text{ fm}^3$ [24, 25] give a constraint of $|e\mathbf{B}| \ll 1.8 \times 10^5 \text{ MeV}^2$, which is a somewhat weaker constraint than from the magnetic moment interaction. A more naive, but still reasonable restriction is that $|e\mathbf{B}| \ll m_\pi^2 \sim 2 \times 10^4 \text{ MeV}^2$ arrived at by requiring nothing more than that “ $|e\mathbf{B}|$ is small”, and it is this more restrictive limit that we adhere to.

III. LATTICE QCD AND BACKGROUND FIELDS

A direct calculation of multi-nucleon processes such as $np \rightarrow d\gamma$ is impossible on a Euclidean space lattice. As briefly mentioned in the introduction, the obstruction is the Maiani-Testa theorem [6] which precludes the calculation of S-matrix elements away from kinematic thresholds in an infinite volume. In principle however, by performing lattice calculations of matrix elements of the relevant electroweak operators at unphysical kinematics in appropriate multi-nucleon states, e.g., $\langle d(\mathbf{p} = 0) | J^\mu | n(\mathbf{p} = 0) p(\mathbf{p} = 0) \rangle$, the undetermined coefficients of the low-energy EFT (modified to accommodate the injection of energy by the lattice) can be determined, leading to an *ab initio* calculation of the low-energy dependence of the process in question. Unfortunately, by present day standards, calculation of such five-point correlators is prohibitively expensive in computational terms. In order to do such a calculation, the two-nucleon (six quark) sources and sinks and the electroweak current operator must be tied together with quark propagators in all possible ways and the corresponding contributions averaged over the ensemble of gauge configurations. Naively, this is one or two orders of magnitude more difficult than computing the NN four-point correlator. Clearly, a more cost-effective solution to this problem is desired.

We will show that calculations of electroweak processes, such as $np \rightarrow d\gamma$ and $\bar{\nu}_e d \rightarrow nne^+$, will be feasible in the near future. Our method is to some extent motivated by the earliest lattice calculations of the magnetic moments of the proton and neutron. Modern

calculations of these quantities are performed by taking nucleon matrix elements of the electromagnetic current operator. However, in the early days of lattice QCD, calculations of nucleon matrix elements were computationally prohibitive (just as multi-nucleon matrix elements are today) and the magnetic moments were first extracted by measuring the shift in the nucleon mass when the lattice is immersed in a background magnetic field [26, 27, 28]. Taking the magnetic field to be constant and aligned along the z -direction, $\mathbf{B} = B_0 \hat{\mathbf{e}}_z$ the nucleon masses are shifted, e.g. the mass of a proton with spin aligned in the direction of the field is

$$M_{p\uparrow}(B_0) = M + \mu_p B_0 + 4\pi \frac{\beta_p}{2} B_0^2 + \mathcal{O}(B_0^3) \quad . \quad (7)$$

However, it is the energy of the nucleon that is measured on the lattice, and when immersed in a background magnetic field the energy eigenstates of the proton in an infinite volume are

$$E_{p\uparrow}^{(n)}(B_0) = M + \frac{|eB_0|}{M} \left(n + \frac{1}{2} \right) + \frac{p_z^2}{2M} + \mu_p B_0 + 4\pi \frac{\beta_p}{2} B_0^2 + \mathcal{O}(B_0^3) \quad , \quad (8)$$

where n is an integer denoting the Landau-level occupied by the proton, and p_z is the momentum of the proton parallel to the magnetic field. For weak magnetic fields, the spin-dependent energy-splitting is proportional to the magnetic moment of the proton, μ_p , while for stronger fields the magnetic polarizability, β_p becomes significant and measurable [29, 30]. To be complete we note that by using background electric fields, electric polarizabilities [31, 32] and the electric dipole moment of the nucleon [33] have been investigated.

To apply a spatially constant background magnetic field aligned in the z -direction in a lattice simulation, one takes a SU(3) gauge-configuration and modifies the link fields by

$$U_\mu(x) \rightarrow U_\mu(x) U_\mu^{ext}(x) \quad , \quad (9)$$

with

$$U_{0,3}^{ext}(x) = 1 \quad U_1^{ext}(x) = e^{+i\beta x_2} \quad U_2^{ext}(x) = e^{-i\beta x_1} \quad , \quad (10)$$

where β is proportional to $eB_0 b^2$ where b is the lattice spacing⁴. A vector potential with periodic boundary conditions in the transverse directions requires that $eB_0 A_{xy}/2\pi \in \mathbb{Z}$, where A_{xy} is the transverse area of the box. This requirement generates large magnetic fields for present day lattices [26, 27, 28], large enough to shift the nucleon mass by $\gtrsim m_\pi$, and thus too strong to be described by EFT($\not\pi$). Not requiring periodic boundary conditions on the vector potential introduces an exceptional plaquette that can be placed wherever it does the least “harm” in the single nucleon case [26, 27, 28]. It remains to be seen if this plaquette can be placed somewhere to have minimal impact on multi-nucleon simulations or if the periodic requirement must be enforced.

For the weak interactions, and in particular for an axial-vector interaction, the left- and right-handed quarks need to be immersed in different background fields. One way to implement this is to use domain-wall (Kaplan [34]) fermions in the simulation and have the background field vary only in the fifth dimension. A background axial field was used in the first lattice calculation of the axial coupling of the nucleon [35].

By applying such background electroweak fields to nucleons in a finite volume, the energy-levels become sensitive to the various one- and two-nucleon electroweak current operators

⁴ We work in the continuum limit, $b \rightarrow 0$, throughout.

that contribute to the deuteron properties and interactions, such as $np \rightarrow d\gamma$, $\bar{\nu}_e d \rightarrow nne^+$ and other related electroweak processes. It is interesting to note that lattice calculations of the energy-levels relevant to the deuteron magnetic (or weak) moment (isoscalar operator) will be more difficult than those impacting isovector processes as they require the evaluation of disconnected diagrams (where the operator does not connect to valence quarks) which are significantly harder to compute, even in the single nucleon sector [36].

As we will discuss later, it will be necessary to work with asymmetric volumes of dimensions $\eta_1 L \otimes \eta_2 L \otimes L$ [37]. The energy-levels of two-particles in an asymmetric volume have been discussed recently [37] and we review this analysis and extend a number of relevant aspects in Appendix A. It is straightforward to show that the locations of the low-lying energy-levels of two-nucleons interacting in an S-wave on an asymmetric lattice are given by the solutions of [2, 3, 4, 5, 37]

$$p \cot \delta - \frac{1}{\pi L} S(\eta_1, \eta_2; \tilde{p}^2) = 0 \quad , \quad (11)$$

where $p \cot \delta$ uniquely describes the infinite-volume S-wave scattering amplitude below inelastic thresholds. The function $S(\eta_1, \eta_2; \tilde{p}^2)$ is given by

$$S(\eta_1, \eta_2; \tilde{p}^2) = \frac{1}{\eta_1 \eta_2} \sum_{\mathbf{n}}^{\Lambda_n} \frac{1}{|\tilde{\mathbf{n}}|^2 - \tilde{p}^2} - 4\pi \Lambda_n \quad , \quad (12)$$

where $|\tilde{\mathbf{n}}|^2 = \frac{1}{\eta_1^2} n_1^2 + \frac{1}{\eta_2^2} n_2^2 + n_3^2$, and the limits of the linearly-divergent, three-dimensional sum are given by the ellipsoid $|\tilde{\mathbf{n}}|^2 \leq \Lambda_n^2$. The energy corresponding to a given value of \tilde{p} is

$$E = \frac{p^2}{M} = \tilde{p}^2 \frac{4\pi^2}{ML^2} \quad . \quad (13)$$

Given the behavior of two-nucleon energy-levels as a function of the volume, the phase shifts (or at least the first few parameters of the effective range expansion $p \cot \delta = -\frac{1}{a} + \frac{r}{2}p^2 + \dots$) can be recovered. To aid in such recovery, one can find analytic, large volume ($L \rightarrow \infty$) expansions for the locations of the energy-eigenstates, as done by Lüscher for the case of $\eta_{1,2} = 1$ [1, 2, 3, 4, 5] and done by Li and Liu [37] for the lowest continuum level in asymmetric volumes. We detail this construction in Appendix A, and give explicit expressions for the large volume locations of the low-lying levels in the two-nucleon sector. A small L expansion of eq. (11) can also be performed [5], though we do not do this here.

It is straightforward to extend this analysis of two-nucleon energy-levels to include a background electroweak field ⁵. The presence of the background fields can give rise to a number of complications such as Landau-levels and mixing of two-nucleon states of differing total spin and isospin. For this reason we shall develop the necessary generalizations of the above formulas as we need them.

⁵ Recently, Bedaque [38] has considered simulating the NN system in a background field that couples to baryon number, but which has vanishing field-strength. It is found that this is equivalent to performing the simulations with twisted boundary conditions on the quark fields, and that the energy-levels of the system are sensitive to the phase difference between the boundaries. This appears to be a promising avenue for future investigations.

The Hamiltonian of a structure-less point particle of charge e , moving in a uniform, time-independent magnetic field in the z -direction is

$$\hat{H} = \frac{|\hat{\mathbf{p}}|^2}{2M} + \frac{1}{2}M\omega^2(\hat{x}^2 + \hat{y}^2) + \frac{eB_0}{2M} \hat{l}_z \quad , \quad (14)$$

where $\omega = |\frac{eB_0}{2M}|$, and \hat{l}_z is the angular momentum operator parallel to the magnetic field. In an infinite volume, the energy-eigenvalues are given by the expression in eq. (8). However, in a finite volume the oscillator potential is bounded above, and for small enough lattices the potential arising from the magnetic field can be treated as a perturbation. Consequently, for a small magnetic field we can work with momentum eigenstates in the transverse direction. Requiring that the energy-shifts due to these magnetic interactions are small compared with the inter-level spacing of the two-nucleon momentum eigenstates in the finite volume gives,

$$|eB_0| \ll \frac{8\sqrt{3}\pi}{L_\perp^2} \quad , \quad (15)$$

where L_\perp is the size of the transverse dimensions. In what follows we work with momentum eigenstates in the transverse directions, and thus are constrained by eq. (15).

IV. DEUTERON MAGNETIC MOMENT : ISOLATING THE TWO-NUCLEON CONTRIBUTION

It is useful to begin with the simplest case to analyze and understand — the deuteron magnetic moment. To isolate the two-nucleon contribution from the one-nucleon contribution (the magnetic moments of the proton and neutron combined in the $S = 1$ channel), the energy-levels of two nucleons interacting in the 3S_1 channel in a finite volume with a background magnetic field in the z -direction, $\mathbf{B} = B_0 \hat{\mathbf{e}}_z$, are computed.

It is obvious from eq. (7) that the $m = \pm 1$ magnetic sub-states of the NN system will have a linear dependence on the magnetic field for small fields. Indeed, the effect of the background magnetic field on the single-nucleon states is to shift their masses from M to

$$\begin{aligned} M_{p\uparrow} &= M - \frac{eB_0}{2M}\kappa_p \quad , \quad M_{p\downarrow} = M + \frac{eB_0}{2M}\kappa_p \\ M_{n\uparrow} &= M - \frac{eB_0}{2M}\kappa_n \quad , \quad M_{n\downarrow} = M + \frac{eB_0}{2M}\kappa_n \quad , \end{aligned} \quad (16)$$

where $\kappa_{p,n}$ are the proton and neutron magnetic moments. These mass-shifts appear as residual mass-terms in the single nucleon propagators that contribute to the infinite-volume NN scattering amplitude, and hence to the position of the energy-levels of two-nucleons in a finite volume⁶. In the weak- B_0 limit contributions to the NN energy-eigenvalues that are quadratic and higher-order in B_0 , such as the nucleon polarizabilities and modifications arising from the eigenstates in the transverse directions being Landau-levels and not momentum plane-waves, can be neglected.

⁶ Only the free-space nucleon mass M is removed by a phase redefinition of the nucleon field in defining the non-relativistic theory. The presence of interactions between different spin and isospin components of the nucleon field prevents a rescaling of each component to completely remove the mass-shifts in eq. (16).

Since it is a non-relativistic system, a simple recipe can be followed to determine the location of the low-lying energy-eigenstates of two nucleons in a background magnetic field in a finite volume [4, 5]. Construct the inverse scattering amplitude in the background magnetic field, replace the continuum momentum-space loop integral (arising from the bubble-diagrams) by a discrete sum over the allowed momenta in the volume and then find the zeros of the real part [4, 5]. It follows directly from this recipe that the location of the $m = \pm 1$ energy-levels are given by the solutions to

$$p \cot \delta_3 - \frac{1}{\pi L} S(\eta_1, \eta_2; \tilde{p}^2 \pm \tilde{u}_0^2) \mp \frac{eB_0}{2} (\tilde{l}_2 - r_3 \kappa_0) = 0 \quad , \quad (17)$$

where $\kappa_0 = \frac{1}{2}(\kappa_p + \kappa_n)$ and $p \cot \delta_3(p^2) = -\frac{1}{a_3} + \frac{r_3}{2}p^2 + \dots$ is the effective range expansion in the 3S_1 channel. The one-nucleon contribution to the location of the NN energy-levels is through the term

$$\tilde{u}_0^2 = \frac{L^2}{4\pi^2} eB_0 \kappa_0 \quad , \quad (18)$$

and through κ_0 in the last term in eq. (17). The one-nucleon and two-nucleon (determined by \tilde{l}_2) terms enter eq. (17) differently. Consequently, the short-distance and the long-distance interactions with a magnetic field can be separated, i.e. \tilde{l}_2 can be isolated from κ_0 on the lattice. Note that the expression in eq. (17) reduces to the expression in eq. (11) in the limit of vanishing magnetic field.

For symmetric lattices with $\eta_{1,2} = 1$, it follows directly from eq. (17) that for $L \gg a_3$ there are two states that become the deuteron $m = \pm 1$ states in the infinite-volume limit, that have energies

$$E_{-1}^{(m=\pm 1)} = -\frac{\gamma_0^2}{M} \left[1 + \frac{12}{\gamma_0 L} \frac{1}{1 - \gamma_0 r_3} e^{-\gamma_0 L} \right] \mp \mu_d B_0 \quad , \quad (19)$$

in a finite-volume. The deuteron magnetic moment at NLO in the EFT is given in eq. (5), but eq. (19) is true at all orders in the expansion. The leading finite-volume corrections in eq. (19) are the same as those at $B_0 = 0$ [5]. Although this gives a clean lattice measurement of the deuteron magnetic moment (itself a very good test of the lattice approach), it does not facilitate a separation between the one- and two-nucleon contributions.

Making an expansion of eq. (17) about the infinite-volume limit, $E = \mp \frac{eB_0 \kappa_0}{M}$, the energies of the first pair of continuum states in the limit where $L \gg a_3$ are

$$E_0^{(m=\pm 1)} = \mp \frac{eB_0}{M} \kappa_0 + \frac{4\pi A_3}{ML^3} \left[1 - c_1 \frac{A_3}{L} + c_2 \left(\frac{A_3}{L} \right)^2 + \dots \right] \quad , \quad (20)$$

where an effective scattering length is defined to be

$$\frac{1}{A_3} = \frac{1}{a_3} \pm \frac{eB_0}{2} \tilde{l}_2 \quad , \quad (21)$$

and the constants $c_{1,2}$ for $\eta_{1,2} = 1$ are given in Table II [2, 3]. The energies of the second pair of continuum states in the limit where $L \gg a_3$ are

$$E_1^{(m=\pm 1)} = \mp \frac{eB_0}{M} \kappa_0 + \frac{4\pi^2}{ML^2} - \frac{24\pi}{ML^3} \frac{1}{p \cot \tilde{\delta}_0} \left(1 + \frac{2\pi c'_1}{L p \cot \tilde{\delta}_0} + \frac{4\pi^2 c'_2}{L^2 (p \cot \tilde{\delta}_0)^2} \right) \quad (22)$$

where

$$p \cot \tilde{\delta}_0 = -\frac{1}{A_3} + \frac{1}{2} r_3 \frac{4\pi^2}{L^2} \quad , \quad (23)$$

the constants $c'_{1,2}$ for $\eta_{1,2} = 1$ are given in Table II [2, 3], and A_3 is defined in eq. (21).

The energies in eqs. (20) and (22) closely resemble the well-known Lüscher formulas [2, 3], with some interesting modifications. The levels receive shifts proportional to κ_0 corresponding to the shifts that two non-interacting nucleons would receive in a magnetic field in an infinite volume. In addition, instead of the physical scattering length entering into the $1/L$ -expansion, it is the effective scattering length, A_3 that appears. The effective scattering length, defined in eq. (21), depends upon the actual scattering length and the short-distance contribution to the NN interaction due to the background magnetic field. These expressions are not entirely unexpected. In the continuum states the nucleons do not “see each other” much, and the short-distance interactions are a perturbation (as is clear from eqs. (20) and (22)). The single particle energies dominate and the short-distance interaction, which is the sum of both the purely strong interaction and that induced by the background field, is inserted perturbatively. Measuring the energies of the continuum levels over a range of lattice volumes will allow for a clean separation between the one-nucleon and two-nucleon contributions to the deuteron magnetic moment.

Given that the 3S_1 channel is very close to its non-trivial fixed point ($a_3 \rightarrow \infty$), most choices of magnetic field will move the system away from the fixed point, and hence $|A_3|$ will typically (i.e., for natural values of \tilde{l}_2 , $|\tilde{l}_2| \sim 1$ fm) be dramatically smaller than $|a_3|$. This suggests that, in principle, lattices even smaller than those discussed in Ref. [5] could be used to study the two-nucleon sector when a background magnetic field is present. However, nature is not as kind as it might have been, suppressing the isoscalar spin-dependent interactions (proportional to \tilde{l}_2) at low-momentum by even more than the naive $1/N_C^{|I-J|}$ obtained in the large- N_C limit [39]. The experimental value of the deuteron magnetic moment $\kappa_d = 0.85741$ is very close to the single particle sum of $2\kappa_0 = 0.87976$ which results in an unnaturally small value of $\tilde{l}_2 = -0.0576$ fm in eq. (5). Therefore, for magnetic fields that allow for an analysis of the two-nucleon sector within EFT(\not{n}), the effective scattering length, A_3 , is only moderately different from the actual scattering length, a_3 . Specifically, for $eB_0 = 10^4$ MeV², A_3 differs from a_3 by 10% (for the physical value of l_2), an amount that should produce observable shifts in the continuum two-particle energy levels calculated in lattice simulations. In fig. 1 the energy-levels of the three lowest-lying $m = \pm 1$ states are shown, along with the analytic expressions in eqs. (19), (20), (22) and their asymmetric generalizations that are valid for $L \gg a_3$.

An interesting “twist” could be applied to the systems we are considering. It is possible that the light-quark masses, m_q , could be tuned to values for which the physical scattering lengths in the 3S_1 or 1S_0 channels, or both, become infinite [40, 41, 42, 43]. As both channels have unnaturally large scattering lengths at the physical values of m_q , only small changes in these masses will be required, and hence the values of the operators in the pionless theory describing the unphysical system, will differ from their physical values by only small amount. An advantage of considering such an unphysical system is that A_3 will depend only on \tilde{l}_2 and its determination on the lattice would provide a measurement of \tilde{l}_2 for the physical theory with a reasonably small systematic uncertainty.

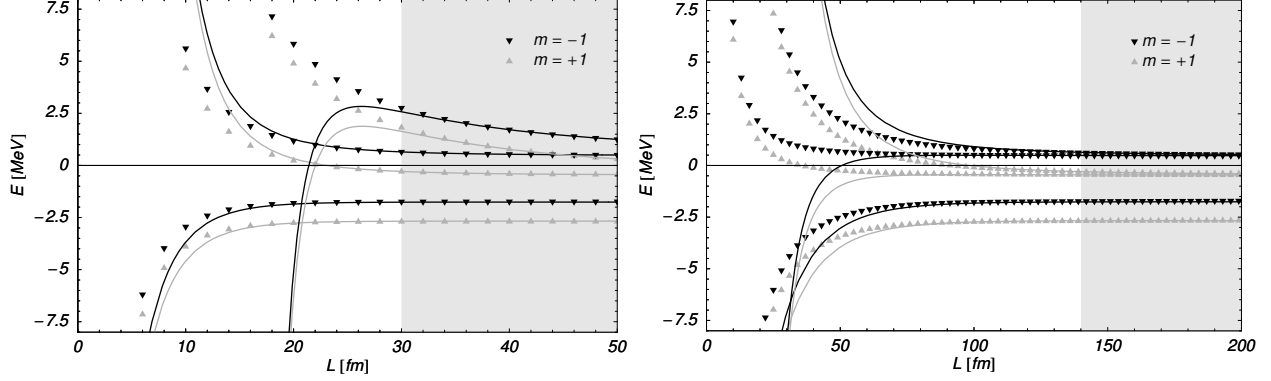


FIG. 1: The energies of the lowest-lying 3S_1 states with $m = \pm 1$ on the lattice as a function of the lattice size, L , in the presence of a background magnetic field of strength $eB_0 = 10^2 \text{ MeV}^2$. The left plot is for a symmetric volume, while the right plot is for $\eta_1 = \eta_2 = 0.2$. The experimental values of the nucleon and deuteron magnetic moments have been used. The two types of triangles correspond to numerical solution of eq. (17), and the curves correspond to the large- L asymptotic behavior given by eqs. (19), (20) and (22) and their asymmetric generalizations. The gray shaded regions denote lattice sizes that are large enough so that the effects of the transverse eigenstates being Landau-levels and not momentum eigenstates cannot be ignored.

V. $np \rightarrow d\gamma$: ISOLATING THE TWO-NUCLEON CONTRIBUTION

The radiative capture process $np \rightarrow d\gamma$, and its inverse reaction (photo-disintegration of the deuteron) provide a classic demonstration of the importance of MEC's in nuclear physics. The one-nucleon contribution to thermal neutron capture provides only $\sim 90\%$ of the experimentally measured cross section. From the EFT perspective, it is natural that two-nucleon electromagnetic interactions can contribute to this process, in the same way that they contribute to the deuteron magnetic moment. The cross sections for $np \rightarrow d\gamma$ for cold neutrons and for the photo-disintegration of the deuteron near threshold are both sensitive to l_1 . The radiative-capture cross section near threshold is given by [22]

$$\sigma(np \rightarrow d\gamma) = \frac{4\pi\alpha (\gamma_0^2 + |\mathbf{p}|^2)^3}{M^4\gamma_0^3|\mathbf{p}|} \left[|\tilde{X}_{M1}|^2 + |\tilde{X}_{E1}|^2 + \dots \right] , \quad (24)$$

where contributions from multipoles other than $M1$ or $E1$, denoted by the ellipses, are parametrically suppressed at low-energies. Near threshold, this process takes the two-nucleons between the 1S_0 channel and the 3S_1 channel and the cross section is dominated by the $M1$ amplitude [44, 45]

$$\tilde{X}_{M1} = \frac{1}{\sqrt{1 - \gamma_0 r_3} - \frac{1}{a_1} + \frac{1}{2}r_1|\mathbf{p}|^2 - i|\mathbf{p}|} \left[\frac{\kappa_1\gamma_0^2}{\gamma_0^2 + |\mathbf{p}|^2} \left(\gamma_0 - \frac{1}{a_1} + \frac{1}{2}r_1|\mathbf{p}|^2 \right) + l_1 \frac{\gamma_0^2}{2} \right] . \quad (25)$$

It is worth stressing that this very simple expression for the cross section (including the analytic form for the $E1$ amplitude [44, 45]) describes all available low-energy data with high precision [10, 44, 45].

A background magnetic field aligned in the z -direction induces a mixing between the 1S_0 , $I_z = 0$ state and 3S_1 , $m = 0$ state. Therefore, the energy-eigenstates in the background field will be a mixture of both the 1S_0 and the 3S_1 channels, which gives rise to quite interesting behavior. In large volumes, the continuum states, for which the strong interactions play only a small role, are perturbatively close to the single particle eigenstates $p^\uparrow n^\downarrow$ and $n^\uparrow p^\downarrow$, with energies dictated by the single particle interactions with the background field, i.e. linear in B_0 for small B_0 . Hence, the energies of the continuum states will be insensitive to the value of l_1 . However, the energies of the near threshold bound-states, the deuteron and the virtual bound di-nucleon state in the 1S_0 channel, for which strong interactions play an important role, will depend quadratically on B_0 for small B_0 and will have sensitivity to l_1 . This results from the fact that these states have equal admixtures of the single particle eigenstates in infinite volumes. Thus, it is clear that we will need to observe energy-shifts that are quadratic in B_0 in order to extract l_1 . This presents a potential problem that we did not encounter for the energy shifts of the $m = \pm 1$ states. In the directions transverse to \mathbf{B} , Landau-levels are the single-particle eigenstates rather than momentum plane-waves. As discussed in section III, this is a complication in infinite volumes, but becomes a far more serious issue in finite volumes for systems with $H(3)$ symmetry. In order to avoid having to contend with this problem, we eliminate it; highly asymmetric lattices, for which $\eta_{1,2} \ll 1$, so as to satisfy eq. (15), strongly suppress excitations in the transverse direction, leaving the system dominated by fluctuations in the z -direction. Ideally, one would take the transverse dimensions almost to zero to eliminate these contributions almost entirely. However, the pion mass sets a lower-limit of $\eta_{1,2}L \sim 2$ fm in order for the pionless theory to provide a valid description. On a symmetric lattice, as studied in Refs. [1, 2, 3, 4, 5], the lowest-lying states are in the A_1 representation of $H(3)$ and as such their energy is dependent upon NN interactions with $J = 0, 4, 6, 8, \dots$ [46] with the notable omission of interactions with $J = 2$. On an asymmetric lattice where $H(3)$ is not a symmetry, NN interactions with even angular momentum will contribute. However, in the power-counting of EFT($\not{\pi}$), higher angular momentum contributions are suppressed and can be systematically included when required.

As the background field induces mixing between the 1S_0 and 3S_1 channels, the energy-eigenvalues are found by diagonalizing the coupled channels system. It is straightforward to show that these eigenvalues are solutions to

$$\left[p \cot \delta_1 - \frac{S_1 + S_2}{2\pi L} \right] \left[p \cot \delta_3 - \frac{S_1 + S_2}{2\pi L} \right] = \left[\frac{eB_0 l_1}{2} + \frac{S_1 - S_2}{2\pi L} \right]^2, \quad (26)$$

where

$$S_1 = S(\eta_1, \eta_2; \tilde{p}^2 + \tilde{u}_1^2), \quad S_2 = S(\eta_1, \eta_2; \tilde{p}^2 - \tilde{u}_1^2), \quad \tilde{u}_1^2 = \frac{L^2}{4\pi^2} eB_0 \kappa_1, \quad (27)$$

$\kappa_1 = (\kappa_p - \kappa_n)/2$ and $p \cot \delta_1 = -\frac{1}{a_1} + \frac{r_1}{2}p^2 + \dots$ is the 1S_0 effective range expansion. The \tilde{u}_1 contributions result from the one-nucleon interactions with the background field, while the two-nucleon-background field interactions are described by l_1 .

The $L \gg a_{1,3}, r_{1,3}$ asymptotic region is more complicated in these mixed channels than in a single channel and we do not have practicable analytic expressions for the energies of the lowest-lying levels in this limit. Thus, all of our intuition and understanding has come about through numerical solution of eq. (26). In fig. 2, we show the spectra of energy-eigenvalues of the $^1S_0(I_z = 0) - ^3S_1(m = 0)$ NN system in magnetic fields of $eB_0 = 4 \times 10^3$ MeV²

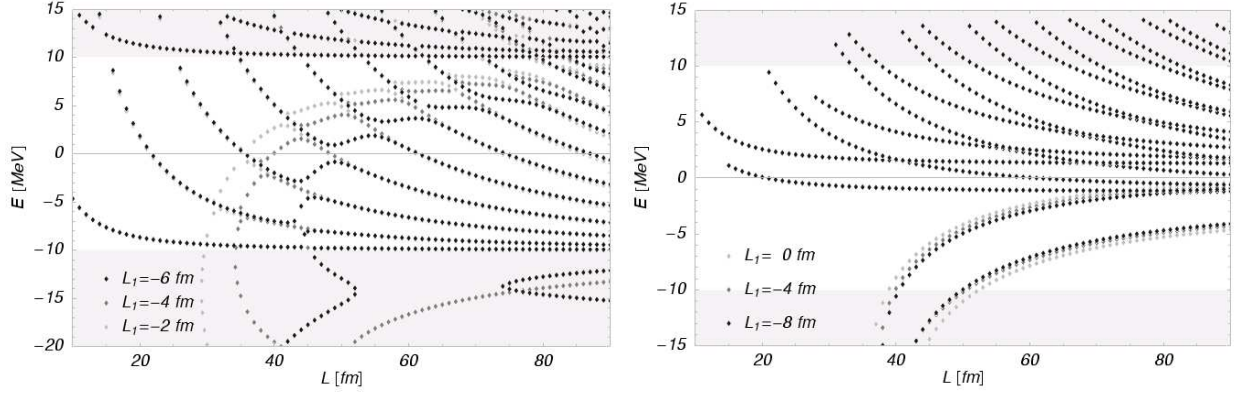


FIG. 2: The energy of the lowest-lying states in the coupled $^1S_0(I_z = 0) - ^3S_1(m = 0)$ channels on an asymmetric lattice with $\eta_{1,2} = 0.1$ as a function of the lattice size, L , in the presence of a background magnetic field. The left panel shows the spectrum for $eB_0 = 4 \times 10^3 \text{ MeV}^2$, while the right panel shows the spectrum for $eB_0 = 5 \times 10^2 \text{ MeV}^2$. The shaded regions indicate energies outside of the $\text{EFT}(\not{\pi})$ and states therein should be treated with extreme caution.

and $eB_0 = 5 \times 10^2 \text{ MeV}^2$ on an asymmetric lattice with $\eta_{1,2} = 0.1$ as a function of lattice size, L . As a function of B_0 and l_1 , the continuum levels behave precisely as one would expect, and are very insensitive to l_1 . However, as anticipated, there are one or two states in the theory (depending on the choice of parameters) which are very sensitive to l_1 . The location of these states in an infinite volume are finely tuned (near the IR fixed point), and as such, “squeezing them” into a volume that is small in the transverse directions destroys this fine-tuning. However, the background field, through the operator with coefficient l_1 , can restore the fine-tuning and make the location of the state depend strongly upon l_1 . Further, the observation of two bound-states in the spectrum that are sensitive to l_1 for some values of background field and for some volumes indicates that the virtual bound state in the 1S_0 channel can be moved onto the first sheet by the background magnetic field. In the infinite volume limit one of the l_1 -dependent states becomes the physical deuteron. However, in a finite volume and in the background field its composition, and the composition of the other states, will be quite complicated, each being a combination of the “deuteron”, the 1S_0 -“dinucleon”, and the continuum states, as deduced from fig. 2. As $\text{EFT}(\not{\pi})$ is applicable only at very low-energies, the energy-spectra in fig. 2 are reliable only for $|E| \lesssim 10 \text{ MeV}$.

For $eB_0 = 4 \times 10^3 \text{ MeV}^2$, as shown in the left panel of fig. 2, there is one “reliable” state⁷ that moves to higher energy as a function of increasing volume, and is very sensitive to l_1 in the physical range of l_1 . For lattice sizes between $\sim 30 \text{ fm}$ and $\sim 50 \text{ fm}$ in the longitudinal direction, this level is one of the low-lying ones in the spectrum, and therefore, somewhat easier to extract from lattice calculations, than if it were high in the spectrum. Also present in this spectrum is the curious feature of “level pair-production” near the cut-off of the theory. In the absence of a background field there are two solutions to eq. (6), one corresponding to the deuteron and one to an unphysical state lying outside the theory,

⁷ By reliable we mean that it lies within the range of validity of $\text{EFT}(\not{\pi})$.

nonetheless both solutions exist, and the one outside the theory is simply discarded as unphysical. The same line of reasoning applies to the deep states in fig. 2. We interpret these states as the unbound di-nucleon state in the 1S_0 channel mixing with continuum states and the deuteron through the background magnetic field, bringing an additional state down from the cut-off into the spectrum. Its sensitivity to l_1 suggests that it is a strongly correlated NN pair, as opposed to predominantly continuum in nature. For $eB_0 = 5 \times 10^2 \text{ MeV}^2$, as shown in the right panel of fig. 2, the two lowest-lying states in the spectrum are both sensitive to l_1 . It might well be the case that a precise measurement of the lowest-lying state in the spectrum at weaker fields is the easiest way to determine l_1 from lattice QCD.

A general statement can be made about the NN system in background magnetic field. There are values of the magnetic field, lattice asymmetry and lattice size for which the spectrum of energy-eigenvalues allows for the short-distance and long-distance contributions to electromagnetic matrix elements to be separated, as is clear from fig. 2. While a lattice extraction of these quantities will be very important to perform and provide a proof in principle of this method, it will not, unfortunately, tell us anything we didn't already know experimentally.

VI. WEAK INTERACTION OBSERVABLES IN THE TWO-NUCLEON SECTOR

Of central importance to present day and future neutrino experiments is the ability to separate the flavors of neutrinos entering the detectors. The method to accomplish this implemented by the SNO collaboration is to use the weak-disintegration of the deuteron, e.g. $\nu_x d \rightarrow \nu_x np$ ($x = e, \mu, \tau$) and $\bar{\nu}_e d \rightarrow nne^+$. These processes “look” like the photo-disintegration of the deuteron discussed in the previous section when the electromagnetic field is replaced by a weak gauge field. There are both one-nucleon and two-nucleon contributions to these processes, but unlike the electromagnetic case, the two-nucleon contributions have significant uncertainties associated (for a nice discussion see Ref. [11]) with them that will impact the future determinations of the neutrino mass and mixing matrices. Therefore a determination of the short-distance contributions to the matrix elements for weak-disintegration of the deuteron from lattice QCD is important.

The procedure for determining the two-nucleon weak interactions is similar to that described in the electromagnetic sector with a few minor differences. For the electromagnetic interactions it sufficed to use a background magnetic field. However, for the weak interactions it is convenient to introduce a fictitious $SU(2)_L \otimes SU(2)_R$ weak gauge symmetry under which the up- and down-quarks transform, giving rise to the interactions

$$\begin{aligned} \mathcal{L}^{\text{int.}} = & -\frac{1}{4} \left[g_L W_{\mu,L}^3 (\bar{u}\gamma^\mu(1 - \gamma_5)u - \bar{d}\gamma^\mu(1 - \gamma_5)d) \right. \\ & \left. + g_R W_{\mu,R}^3 (\bar{u}\gamma^\mu(1 + \gamma_5)u - \bar{d}\gamma^\mu(1 + \gamma_5)d) \right] \quad , \end{aligned} \quad (28)$$

and give vevs to $W_{z,L}^3$ and $W_{z,R}^3$, such that $\langle g_L W_{z,L}^3 \rangle = -\langle g_R W_{z,R}^3 \rangle = gW$. Therefore, in this background weak field there is an additional contribution to the strong interaction Lagrange density of

$$\delta\mathcal{L} = -\frac{1}{2}gW (\bar{u}\gamma^z\gamma_5u - \bar{d}\gamma^z\gamma_5d) \quad . \quad (29)$$

This interaction leads to interactions in the di-baryon formulation of EFT($\not{\pi}$) of the form

$$\delta\mathcal{L} = -gW \frac{g_A}{2} N^\dagger \sigma^z \tau^3 N - \frac{gW l_{1,A}}{2M\sqrt{r_1 r_3}} \left[t_3^\dagger s_3 + \text{h.c.} \right] + \dots, \quad (30)$$

where the ellipses denotes terms higher order in EFT($\not{\pi}$), and $g_A = 1.26$ is the nucleon axial coupling constant. We note that due to the nature of the interaction, weak “Landau-levels” are not present in this system.

The cross sections for the weak-disintegration of the deuteron and other two-nucleon weak processes depend upon the dimensionless coefficient $l_{1,A}$. These processes have been studied extensively by Butler and Chen [47, 48] and also by Butler, Chen and Kong [49] and our (renormalization-group invariant) $l_{1,A}$ is related to the constants they introduce. The coefficient of the four-nucleon operator in EFT($\not{\pi}$), ${}^\#L_{1,A}$, is related to $l_{1,A}$ via

$$l_{1,A} = -\frac{2(\mu - \gamma)}{C_0^{({}^1S_0)}(\mu)} \left[{}^\#L_{1,A}(\mu) - \pi g_A \left(\frac{M}{2\pi} C_2^{({}^1S_0)}(\mu) + \frac{r_3}{(\mu - \gamma)^2} \right) \right], \quad (31)$$

where $C_{0,2}^{({}^1S_0)}(\mu)$ are the coefficients of the zero- and two-derivative strong interaction operators in EFT($\not{\pi}$). Numerically, eq. (31) reduces to

$$l_{1,A} = -13.4 + 0.27 {}^\#L_{1,A}, \quad (32)$$

when the RG-scale $\mu = m_\pi$ is chosen, and where ${}^\#L_{1,A}$ is in units of fm^3 . Calculations have been done in which a chiral expansion of the weak currents are performed in a manner consistent with Weinberg’s power-counting [50]. Matrix elements of these operators are taken between wave-functions generated with the best modern NN potentials [13]. This method is somewhat *ad hoc*, but it has been demonstrated to be convergent where it has been tested. A calculation of tritium β -decay in such a framework leads to [13] ${}^\#L_{1,A}(m_\pi) = +4.2 \pm 0.1 \text{ fm}^3$. Chen, Heeger and Robertson [11] have surveyed the experimental and theoretical constraints on ${}^\#L_{1,A}(m_\pi)$ and have also provided a model-independent determination of this quantity from the SNO and Super-Kamiokande data, finding ${}^\#L_{1,A} = +4.0 \pm 6.3 \text{ fm}^3$.

The cross sections for the processes $\nu d \rightarrow \nu np$, $\bar{\nu} d \rightarrow \bar{\nu} np$, and $\bar{\nu} d \rightarrow e^+ nn$ are all given in terms of ${}^\#L_{1,A}(m_\pi)$, in Refs. [47, 48, 49], and analytic expressions for each can be found there. As these expressions are quite complicated, we do not reproduce them here. Numerical values of the cross sections for these processes can be found in Refs. [47, 48, 49]. As an example, at $E_{\nu, \bar{\nu}} = 10 \text{ MeV}$ the cross sections are, in units of 10^{-42} cm^2 ,

$$\begin{aligned} \sigma(\nu_x d \rightarrow \nu_x np) &= 1.76 + 0.056 l_{1,A}, \quad \sigma(\bar{\nu}_x d \rightarrow \bar{\nu}_x np) = 1.66 + 0.052 l_{1,A} \\ \sigma(\nu_e d \rightarrow e^- pp) &= 4.07 + 0.12 l_{1,A}, \quad \sigma(\bar{\nu}_e d \rightarrow e^+ nn) = 1.93 + 0.059 l_{1,A}, \end{aligned} \quad (33)$$

where $x = e, \mu, \tau$. Thus, a determination of $l_{1,A}$ at the $\sim 10\%$ level translates into an uncertainty in these cross sections at the few percent level.

In the presence of a background weak field of the form given in eqs. (29) and (30), the $I_z = 0$ component of the 1S_0 channel mixes with the $m = 0$ component of the 3S_1 channel, as is the case in the presence of a background magnetic field. The energy-eigenvalues of ${}^1S_0(I_z = 0) - {}^3S_1(m = 0)$ NN system in a finite volume with this weak field are solutions to

$$\left[p \cot \delta_1 - \frac{S_1 + S_2}{2\pi L} \right] \left[p \cot \delta_3 - \frac{S_1 + S_2}{2\pi L} \right] = \left[\frac{gW l_{1,A}}{4} - \frac{S_1 - S_2}{2\pi L} \right]^2, \quad (34)$$

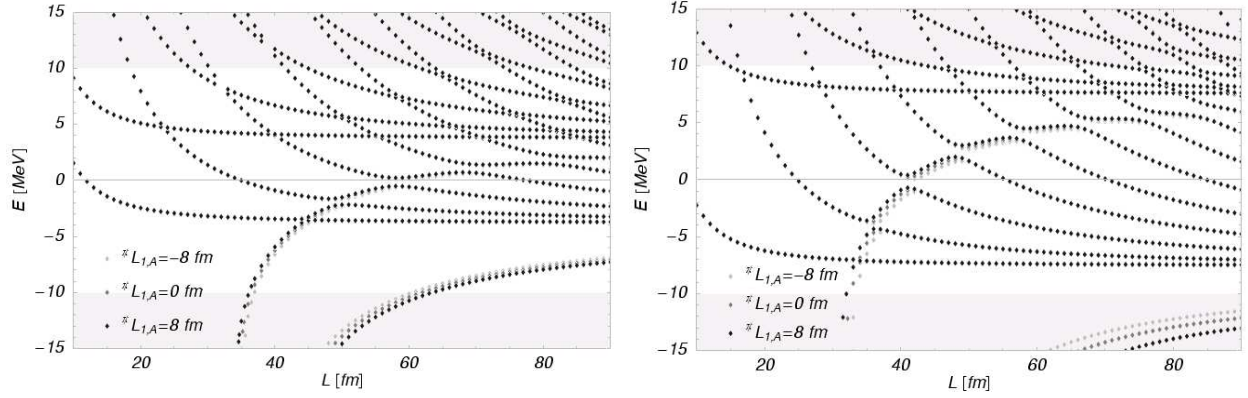


FIG. 3: The energy of the lowest-lying states in the coupled $^1S_0(I_z = 0) - ^3S_1(m = 0)$ channels on an asymmetric lattice with $\eta_{1,2} = 0.1$ as a function of the lattice size, L , in the presence of a background weak field. The left panel shows the spectrum in the presence of a background field $gW = 3$ MeV, while the right panel shows the spectrum for $gW = 6$ MeV. The shaded regions indicate energies outside of the EFT(π) and states therein should be treated with extreme caution.

where

$$S_1 = S(\eta_1, \eta_2; \tilde{p}^2 + \tilde{w}_1^2) \quad , \quad S_2 = S(\eta_1, \eta_2; \tilde{p}^2 - \tilde{w}_1^2) \quad , \quad \tilde{w}_1^2 = -\frac{L^2}{4\pi^2} gW g_A M \quad . \quad (35)$$

In analogy with the electromagnetic case, the \tilde{w}_1 contributions result from the one-nucleon interactions with the background weak field, while the two-nucleon interactions are described by $l_{1,A}$. As in the electromagnetic case, we have explored the spectrum of this system through numerical solution of eq. (35). The spectra of two-nucleons in background weak fields of strengths $gW = 3$ MeV and $gW = 6$ MeV are shown in fig. 3 as a function of L . In complete analogy with the electromagnetic case, the continuum levels are insensitive to $l_{1,A}$, while there is one level, or two levels for some parameters, that are sensitive to $l_{1,A}$ due to the fine-tuning in the NN sector. For lattices with size $L \sim 40$ fm and $\eta_{1,2} = 0.1$ the state that is sensitive to $l_{1,A}$ is either the lowest state or one of the lowest states, depending upon the choice of field. Over a reasonable range of $l_{1,A}$, the energies of the levels that are sensitive to $l_{1,A}$ vary by ~ 1 MeV, which should be measurable.

It is also worth pointing out that an asymmetric lattice is not necessary to study these weak interactions. It is the existence of Landau-levels in the case of a magnetic field that forced us to consider an asymmetric lattice to suppress excitations in the transverse directions. However, for the weak background field in eqs. (29) and (30) the transverse eigenstates are momentum eigenstates, and as such a symmetric lattice is sufficient.

It is clear from fig. 3 that such lattice simulations of two-nucleons in a background weak field will allow for a determination of $l_{1,A}$. We find this to be quite remarkable. As a final comment on the weak properties of the two-nucleon sector, one could explore the weak-moment of the deuteron. This too will have contributions from the weak-moments of the nucleons, and also from short-distance interactions with the neutral-current gauge-field. By examining the two-nucleon spectrum in the presence of an isoscalar weak field, the short-distance interaction could be isolated from the long-distance contribution and the deuteron

weak moment could be determined. This too would be a spectacular accomplishment for lattice QCD.

VII. CONCLUSIONS

In this work we have shown that lattice simulations of the two-nucleon sector in a finite volume and in the presence of background electroweak fields allow for the isolation of the short-distance, multi-nucleon electroweak currents, traditionally called “meson-exchange currents”. In lattice QCD simulations one has many more “knobs” to turn to get at the physics one is interested in. In particular, the dimensions of the lattice can be chosen to disturb the fine-tuning in the two-nucleon sector in a controlled way to maximize sensitivity to the short-distance electroweak interactions. Remarkably, there can be one or two levels in the spectrum that are highly sensitive to these short-distance interactions, while the continuum states show little sensitivity. Consequently, for some background fields and lattice dimensions, the short-distance interactions can be isolated from the long-distance interactions.

One would like to see a higher-order analysis of these finite volume observables in EFT(π) including the effects of the Landau-levels, one- and two-nucleon polarizabilities and other relevant contributions. Further, our analysis has been performed exclusively with the pionless EFT, EFT(π). While the results are rigorous where applicable, this work needs to be extended to a larger range of energies and momenta, which requires solving the pionful theory in a finite volume. Progress toward this goal is being made in the zero- and single nucleon sectors, but so far little progress has been made in the multi-nucleon sectors. Recently, Lee, Borasoy and Schaefer [51] have performed the first lattice simulations of the pionful EFT using Weinberg’s power-counting, with an eye to a complete numerical solution of multi-nucleon systems⁸. Further, encouraging progress has been made toward setting-up lattice simulations in EFT(π) [54, 55].

The numerical analysis we have presented in this work has been for the physical values of the strong interaction parameters, and consequently, for the physical values of the quark masses. Lattice simulations of the immediate future will not be performed at the physical quark masses, be they quenched, partially-quenched⁹ or unquenched. It is possible that the scattering lengths in these unphysical simulations will not be unnaturally large, and the pionless theory will not be applicable. Therefore, it is more than likely that the pionful theory will need to be solved to more precisely understand how the scattering parameters depend upon the light quark masses, and to directly extract the interactions that result from physics at the cut-off scale of the pionful theory.

This work provides the first steps toward extracting the electromagnetic and weak properties of nuclei from lattice QCD simulations. We encourage lattice practitioners to explore this new area and to determine the resources required to perform such calculations. As mentioned earlier, even if infinite computing power were presently available, one knows very

⁸ The formal problems associated with the chiral expansion in Weinberg’s power-counting uncovered in Ref. [52] (see also Ref. [53]) have not been resolved in Ref. [51].

⁹ Generically, the non-unitary nature of the quenched and partially-quenched versions of QCD is problematic when considering two-particle scattering. However, for energies below ghost meson production threshold, the partially-quenched theory is unitary and can be analyzed rigorously [56].

little about what to compute in lattice QCD in order to make predictions about nuclear processes. Therefore, we encourage nuclear theorists to extend this work and the work of Refs. [1, 2, 3, 4, 5] so that a rigorous computational framework for nuclear physics is in place when the computing power becomes available.

Acknowledgments

We would like to thank Silas Beane, Paulo F. Bedaque, David B. Kaplan, David Lin, Assumpta Parreno, Steve Sharpe and Matt Wingate for numerous discussions. Further, we thank the other members of the NPLQCD effort for useful input.

APPENDIX A: TWO NUCLEONS ON AN ASYMMETRIC LATTICE

The energy-levels and formalism associated with two interacting particles on an asymmetric lattice of finite volume, have recently been studied [37]. We use the asymmetric lattice to suppress nucleon momentum modes in the directions transverse to the background magnetic field in order to extract the electromagnetic counterterm, \tilde{l}_2 , i.e. to minimize the contribution from the $N^\dagger \mathbf{A} \cdot \nabla N$ and $N^\dagger \mathbf{A}^2 N$ interactions which generate Landau-levels in an infinite volume.

Explicit evaluation of the function $S(\eta_1, \eta_2; \tilde{p}^2)$ defined in eqs. (11) and (12) can be accomplished in a variety of ways. Extending the Chowla-Selberg relation [57] to asymmetric lattices, it is easy to show that for $x \gtrsim 0$

$$S(\eta_1, \eta_2; -x^2) = -2\pi^2 x + \pi \sum_{\mathbf{m} \neq \mathbf{0}} \frac{1}{|\mathbf{m}|} e^{-2\pi |\mathbf{m}| x} , \quad (\text{A1})$$

where $|\mathbf{m}|^2 = \eta_1^2 m_1^2 + \eta_2^2 m_2^2 + m_3^2$. In order to facilitate evaluation of $S(\eta_1, \eta_2; \tilde{p}^2)$, and also to determine the coefficients in the expansion of the energy-levels as a function of lattice size, three sums are evaluated for a given lattice asymmetry. The most convergent sum ($\sim 1/\Lambda_n^3$ in the UV) is

$$K_{\eta_1 \eta_2} = \frac{1}{\eta_1 \eta_2} \sum_{\mathbf{n} \neq \mathbf{0}} \frac{1}{|\tilde{\mathbf{n}}|^6} . \quad (\text{A2})$$

A second sum is

$$\begin{aligned} J_{\eta_1 \eta_2} &= \frac{1}{\eta_1 \eta_2} \sum_{\mathbf{n} \neq \mathbf{0}} \frac{1}{|\tilde{\mathbf{n}}|^4} \\ &= \frac{\pi^2}{x} \left[1 + \sum_{\mathbf{m} \neq \mathbf{0}} e^{-2\pi |\mathbf{m}| x} \right] - \frac{1}{\eta_1 \eta_2 x^4} + \frac{1}{\eta_1 \eta_2} \sum_{\mathbf{n} \neq \mathbf{0}} \frac{2x^2 |\tilde{\mathbf{n}}|^2 + x^4}{|\tilde{\mathbf{n}}|^4 (|\tilde{\mathbf{n}}|^2 + x^2)^2} , \end{aligned} \quad (\text{A3})$$

and it is important to note that $J_{\eta_1 \eta_2}$ is independent of the value of x , and the expression in eq. (A3) holds for $x \gtrsim 0$, and also converges as $\sim 1/\Lambda_n^3$. The third sum is

$$I_{\eta_1 \eta_2} = \lim_{\Lambda_n \rightarrow \infty} \left[\frac{1}{\eta_1 \eta_2} \sum_{\mathbf{n} \neq \mathbf{0}}^{\Lambda_n} \frac{1}{|\tilde{\mathbf{n}}|^2} - 4\pi \Lambda_n \right]$$

$$\begin{aligned}
&= -2\pi^2 x + \pi \sum_{\mathbf{m} \neq \mathbf{0}} \frac{1}{|\mathbf{m}|} e^{-2\pi|\mathbf{m}|x} - \frac{1}{\eta_1 \eta_2 x^2} + x^2 J_{\eta_1 \eta_2} - x^4 K_{\eta_1 \eta_2} \\
&\quad + \frac{x^6}{\eta_1 \eta_2} \sum_{\mathbf{n} \neq \mathbf{0}} \frac{1}{|\tilde{\mathbf{n}}|^6 (|\tilde{\mathbf{n}}|^2 + x^2)} \quad , \tag{A4}
\end{aligned}$$

which is also independent of the value of x , and the expression in eq. (A4) holds for $x \gtrsim 0$. The numerical values of these sums are given in Table I for different lattice asymmetries $\eta_{1,2}$. In terms of these \tilde{p} -independent constants, the function $S(\eta_1, \eta_2; \tilde{p}^2)$ can be written as

TABLE I: The constants $I_{\eta_1 \eta_2}$, $J_{\eta_1 \eta_2}$, $K_{\eta_1 \eta_2}$ for different lattice asymmetries η_1, η_2 .

η_1, η_2	$I_{\eta_1 \eta_2}$	$J_{\eta_1 \eta_2}$	$K_{\eta_1 \eta_2}$
0.1 , 0.1	206.456	217.884	203.475
0.2 , 0.2	20.9815	56.9542	50.9151
1 , 1	-8.91368	16.5323	8.40191

$$S(\eta_1, \eta_2; \tilde{p}^2) = I_{\eta_1 \eta_2} - \frac{1}{\eta_1 \eta_2 \tilde{p}^2} + \tilde{p}^2 J_{\eta_1 \eta_2} + \frac{\tilde{p}^4}{\eta_1 \eta_2} \sum_{\mathbf{n} \neq \mathbf{0}}^{\Lambda_n} \frac{1}{|\tilde{\mathbf{n}}|^4 (|\tilde{\mathbf{n}}|^2 - \tilde{p}^2)} \quad , \tag{A5}$$

which is valid for all lattices defined by $\eta_{1,2}$, and for all \tilde{p}^2 . Accuracy in the 5th or 6th significant digit can be obtained by evaluating a few finite sums that require insignificant amounts of computer time. An additional check on our numerics is provided by the integral representation

$$\begin{aligned}
S(\eta_1, \eta_2; \tilde{p}^2) &= 2\pi^{3/2} e^{\tilde{p}^2} (2\tilde{p}^2 - 1) + \frac{e^{\tilde{p}^2}}{\eta_1 \eta_2} \sum_{\mathbf{n}} \frac{e^{-|\tilde{\mathbf{n}}|^2}}{|\tilde{\mathbf{n}}|^2 - \tilde{p}^2} \\
&\quad - \pi^{3/2} \int_0^1 dt \frac{e^{t\tilde{p}^2}}{t^{3/2}} \left(4\tilde{p}^4 t^2 - \sum_{\mathbf{m} \neq \mathbf{0}} e^{\frac{-\pi^2 |\mathbf{m}|^2}{t}} \right) \quad . \tag{A6}
\end{aligned}$$

In the limit that all lattice dimensions are much larger than any strong interaction length scale, including the scattering length, approximate formula for the energy-levels can be found [1, 2, 3]. An expression for the energy of the first continuum state of two particles on an asymmetric lattice has been given in this large-volume limit in Ref. [37], and we add to this work by giving expressions for the bound state (the deuteron) and for the second continuum level. We find that the bound state energy of two nucleons in the 3S_1 channel is

$$E_{-1}^{(^3S_1)} = \frac{\gamma_0^2}{M} \left[1 + \frac{4}{\gamma_0 L (1 - \gamma_0 r_3)} \left(e^{-\gamma_0 L} + \frac{1}{\eta_1} e^{-\gamma_0 \eta_1 L} + \frac{1}{\eta_2} e^{-\gamma_0 \eta_2 L} \right) \right] \quad . \tag{A7}$$

In the relevant case of $\eta_{1,2} \ll 1$, the first term in the round brackets can be neglected and the second two dominate the expression (for other cases such as $\eta_{1,2} \gg 1$ the modifications are obvious). Physically, the dominance of the transverse dimensions is reasonable for $\eta_{1,2} \ll 1$ as the contributions to the kinetic energy of the nucleons in the deuteron from these two directions are being reduced, moving the deuteron further from its infrared fixed-point. As

expected for an attractive interaction, the deuteron becomes more deeply bound as the lattice volume is reduced.

The energy of the lowest-lying continuum state, corresponding to the lowest momentum mode in all three directions, is

$$E_0 = \frac{4\pi a}{\eta_1 \eta_2 M L^3} \left[1 - c_1(\eta_1, \eta_2) \left(\frac{a}{L} \right) + c_2(\eta_1, \eta_2) \left(\frac{a}{L} \right)^2 + \dots \right] \quad , \quad (\text{A8})$$

valid in both the 1S_0 and 3S_1 channels. The values of the coefficients c_1 and c_2 for various values of $\eta_{1,2}$ are given in Table II.

TABLE II: Values of the constants $c_{1,2}(\eta_1, \eta_2)$ and $c'_{1,2}(\eta_1, \eta_2)$ for different lattice asymmetries η_1, η_2 . Additional values of $c_{1,2}(\eta_1, \eta_2)$ are given in Ref. [37].

η_1, η_2	$c_1(\eta_1, \eta_2)$	$c_2(\eta_1, \eta_2)$	$c'_1(\eta_1, \eta_2)$	$c'_2(\eta_1, \eta_2)$	d
0.1 , 0.1	65.7171	2111.12	-3.60224	-52.944	1
0.2 , 0.2	6.67861	-99.6627	-2.3242	0.950737	1
0.5 , 0.5	-3.61168	6.65945	0.73400	0.24642	1
1 , 1	-2.837297	6.375183	-0.061367	-0.354156	3

The next continuum level corresponds to non-zero momentum in the longest direction(s), e.g. $\mathbf{p} = (0, 0, \pm \frac{2\pi}{L})$ for $\eta_{1,2} \leq 1$. For large L , the energy of this level for $\eta_{1,2} \leq 1$ is

$$E_1 = \frac{4\pi^2}{ML^2} - d \frac{4 \tan \delta_0}{\eta_1 \eta_2 M L^2} [1 + c'_1(\eta_1, \eta_2) \tan \delta_0 + c'_2(\eta_1, \eta_2) \tan \delta_0 + ..] \quad , \quad (\text{A9})$$

where the phase shift is evaluated at $|\mathbf{p}|^2 = 4\pi^2/L^2$, and d is a degeneracy factor, given in Table II. Again for other choices of $\eta_{1,2}$, the corresponding expressions are easily derived. Values of the coefficients $c'_{1,2}$ are given in Table II for some choices of $\eta_{1,2}$. The large values of some of the c_i 's in Table II indicate that it is the “short” direction(s) that are setting the scale of the finite-volume corrections, and not the “long” direction(s).

Finally we note that there are curves in the η_1 - η_2 plane for which $c_{1,2}(\eta_1, \eta_2)$ separately vanish, as shown in fig. 4. The point on this plot that is most relevant to our analysis is $\eta_1 = \eta_2 = 0.268494$ for which $c_1 = 0$. Such “magic boxes” may prove to be useful in lattice calculations as the asymptotic formulas in eqs. (A7)–(A9) have better convergence properties at smaller L than those associated with arbitrary lattice volumes. Analogous contours exist for the $c'_{1,2}(\eta_1, \eta_2)$ in the η_1 - η_2 plane.

-
- [1] K. Huang and C.N. Yang, *Phys. Rev.* **105**, 767 (1957).
 - [2] M. Lüscher, *Commun. Math. Phys.* **105** 153 (1986).
 - [3] M. Lüscher, *Nucl. Phys.* **B354**, 531 (1991).
 - [4] S. R. Beane, P. F. Bedaque, A. Parreno and M. J. Savage, arXiv:nucl-th/0311027.
 - [5] S. R. Beane, P. F. Bedaque, A. Parreno and M. J. Savage, arXiv:hep-lat/0312004.
 - [6] L. Maiani and M. Testa, *Phys. Lett.* **B245**, 585 (1990).
 - [7] S. Aoki *et al.* [CP-PACS Collaboration], *Phys. Rev.* **D67**, 014502 (2003), hep-lat/0209124.

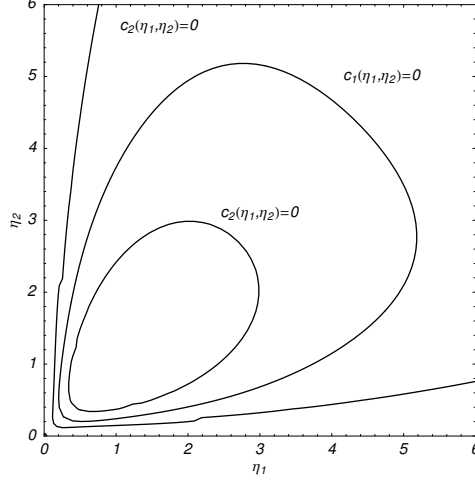


FIG. 4: Curves in the $\eta_1\eta_2$ plane for which $c_{1,2}(\eta_1, \eta_2)$ vanish.

- [8] M. Fukugita, Y. Kuramashi, M. Okawa, H. Mino and A. Ukawa, *Phys. Rev.* **D52**, 3003 (1995), [hep-lat/9501024](#).
- [9] H.R. Fiebig and H. Markum, [hep-lat/0212037](#).
- [10] W. Tornow *et al.*, *Phys. Lett.* **B574**, 8 (2003), [nucl-ex/0309009](#).
- [11] J.W. Chen, K.M. Heeger and R.G.H. Robertson, *Phys. Rev.* **C67**, 025801 (2003), [nucl-th/0210073](#).
- [12] M. Butler, J.W. Chen and P. Vogel, *Phys. Lett.* **B549**, 26 (2002), [nucl-th/0206026](#).
- [13] T.S. Park *et al.*, *Phys. Rev.* **C67**, 055206 (2003), [nucl-th/0208055](#).
- [14] Q. R. Ahmad *et al.* [SNO Collaboration], *Phys. Rev. Lett.* **89**, 011301 (2002) [[arXiv:nucl-ex/0204008](#)].
- [15] D. B. Kaplan, M. J. Savage and M. B. Wise, *Phys. Lett. B* **424**, 390 (1998) [[arXiv:nucl-th/9801034](#)].
- [16] D. B. Kaplan, M. J. Savage and M. B. Wise, *Nucl. Phys. B* **534**, 329 (1998) [[arXiv:nucl-th/9802075](#)].
- [17] U. van Kolck, *Nucl. Phys. A* **645**, 273 (1999) [[arXiv:nucl-th/9808007](#)].
- [18] J. W. Chen, G. Rupak and M. J. Savage, *Nucl. Phys. A* **653**, 386 (1999) [[arXiv:nucl-th/9902056](#)].
- [19] M. C. Birse, J. A. McGovern and K. G. Richardson, *Phys. Lett. B* **464**, 169 (1999) [[arXiv:hep-ph/9807302](#)].
- [20] M. C. Birse, J. A. McGovern and K. G. Richardson, [arXiv:hep-ph/9808398](#).
- [21] D. B. Kaplan, *Nucl. Phys. B* **494**, 471 (1997) [[arXiv:nucl-th/9610052](#)].
- [22] S. R. Beane and M. J. Savage, *Nucl. Phys. A* **694**, 511 (2001) [[arXiv:nucl-th/0011067](#)].
- [23] D. B. Kaplan, M. J. Savage and M. B. Wise, *Phys. Rev. C* **59**, 617 (1999) [[arXiv:nucl-th/9804032](#)].
- [24] V. Olmos de Leon *et al.*, *Eur. Phys. J. A* **10** (2001) 207.
- [25] M. Lundin *et al.*, *Phys. Rev. Lett.* **90**, 192501 (2003) [[arXiv:nucl-ex/0204014](#)].
- [26] G. Martinelli, G. Parisi, R. Petronzio and F. Rapuano, *Phys. Lett. B* **116**, 434 (1982).
- [27] C. W. Bernard, T. Draper, K. Olynyk and M. Rushton, *Phys. Rev. Lett.* **49**, 1076 (1982);
C. W. Bernard, T. Draper and K. Olynyk, *Nucl. Phys. B* **220**, 508 (1983).

- [28] H. R. Rubinstein, S. Solomon and T. Wittlich, Nucl. Phys. B **457**, 577 (1995); H. R. Rubinstein, S. Solomon and T. Wittlich, Nucl. Phys. Proc. Suppl. **42**, 358 (1995).
- [29] L. Zhou, F. X. Lee, W. Wilcox and J. Christensen, Nucl. Phys. Proc. Suppl. **119**, 272 (2003).
- [30] M. Burkardt, D. B. Leinweber and X. m. Jin, Phys. Lett. B **385**, 52 (1996).
- [31] H. R. Fiebig, W. Wilcox and R. M. Woloshyn, Nucl. Phys. B **324**, 47 (1989).
- [32] J. Christensen, F. X. Lee, W. Wilcox and L. m. Zhou, Nucl. Phys. Proc. Suppl. **119**, 269 (2003) [arXiv:hep-lat/0209043].
- [33] S. Aoki and A. Gocksch, Phys. Rev. Lett. **63**, 1125 (1989) [Erratum-ibid. **65**, 1172 (1990)]; S. Aoki, A. Gocksch, A. V. Manohar and S. R. Sharpe, Phys. Rev. Lett. **65**, 1092 (1990).
- [34] D. B. Kaplan, Phys. Lett. B **288**, 342 (1992) [arXiv:hep-lat/9206013].
- [35] F. Fucito, G. Parisi and S. Petrarca, Phys. Lett. B **115**, 148 (1982).
- [36] S. Güsken, arXiv:hep-lat/9906034.
- [37] X. Li and C. Liu, arXiv:hep-lat/0311035.
- [38] P. F. Bedaque, arXiv:nucl-th/0402051.
- [39] D. B. Kaplan and M. J. Savage, Phys. Lett. B **365**, 244 (1996) [arXiv:hep-ph/9509371].
- [40] S. R. Beane and M. J. Savage, Nucl. Phys. A **713**, 148 (2003) [arXiv:hep-ph/0206113].
- [41] S. R. Beane and M. J. Savage, Nucl. Phys. A **717**, 91 (2003) [arXiv:nucl-th/0208021].
- [42] E. Epelbaum, U. G. Meissner and W. Glockle, Nucl. Phys. A **714**, 535 (2003) [arXiv:nucl-th/0207089].
- [43] E. Braaten and H. W. Hammer, Phys. Rev. Lett. **91**, 102002 (2003) [arXiv:nucl-th/0303038].
- [44] J. W. Chen and M. J. Savage, Phys. Rev. C **60**, 065205 (1999) [arXiv:nucl-th/9907042].
- [45] G. Rupak, Nucl. Phys. A **678**, 405 (2000) [arXiv:nucl-th/9911018].
- [46] J.E. Mandula, G. Zweig and J. Govaerts, *Nucl. Phys.* **B228**, 91 (1983).
- [47] M. Butler and J. W. Chen, Nucl. Phys. A **675**, 575 (2000) [arXiv:nucl-th/9905059].
- [48] M. Butler and J. W. Chen, Phys. Lett. B **520**, 87 (2001) [arXiv:nucl-th/0101017].
- [49] M. Butler, J. W. Chen and X. Kong, Phys. Rev. C **63**, 035501 (2001) [arXiv:nucl-th/0008032].
- [50] S. Weinberg, Phys. Lett. B **251**, 288 (1990); Nucl. Phys. B **363**, 3 (1991).
- [51] D. Lee, B. Borasoy, T. Schaefer, [arXiv:nucl-th/0402072].
- [52] D. B. Kaplan, M. J. Savage and M. B. Wise, Nucl. Phys. B **478**, 629 (1996) [arXiv:nucl-th/9605002].
- [53] S. R. Beane, P. F. Bedaque, M. J. Savage and U. van Kolck, Nucl. Phys. A **700**, 377 (2002) [arXiv:nucl-th/0104030].
- [54] H. M. Muller, S. E. Koonin, R. Seki and U. van Kolck, Phys. Rev. C **61**, 044320 (2000) [arXiv:nucl-th/9910038].
- [55] J. W. Chen and D. B. Kaplan, arXiv:hep-lat/0308016.
- [56] S. R. Beane and M. J. Savage, Phys. Rev. D **67**, 054502 (2003) [arXiv:hep-lat/0210046].
- [57] E. Elizalde, *Commun. Math. Phys.* **198**, 83 (1998), hep-th/9707257.